Modeling of a Magneto-Rheological (MR) Fluid Damper using a Self Tuning Fuzzy Mechanism

Kyoung Kwan Ahn*, Dinh Quang Truong, Muhammad Aminul Islam
School of Mechanical and Automotive Engineering, University of Ulsan, San 29, Muger 2dong, Nam-gu, Ulsan, 680-764, Korea

Abstract
A magneto-rheological (MR) fluid damper is a semi-active control device that has recently begun to receive more attention in the vibration control community. However, the inherent nonlinear nature of the MR fluid damper makes it challenging to use this device to achieve high damping control system performance. Therefore the development of an accurate modeling method for a MR fluid damper is necessary to take advantage of its unique characteristics. Our goal was to develop an alternative method for modeling a MR fluid damper by using a self tuning fuzzy (STF) method based on neural technique. The behavior of the researched damper is directly estimated through a fuzzy mapping system. In order to improve the accuracy of the STF model, a back propagation and a gradient descent method are used to train online the fuzzy parameters to minimize the model error function. A series of simulations had been done to validate the effectiveness of the suggested modeling method when compared with the data measured from experiments on a test rig with a researched MR fluid damper. Finally, modeling results show that the proposed STF interference system trained online by using neural technique could describe well the behavior of the MR fluid damper without need of calculation time for generating the model parameters.

Keywords: Magneto-Rheological (MR) Fluid, Damper, Modeling, Self Tuning, Fuzzy

1. Introduction

Nowadays many kinds of actuator was developed and widely used in industry. Among them, the magnetic actuator has only been considered and studied since the 1960s. However, it has proved the advantages, reliabilities and flexibilities in the real applications. Recently, many researchers have been conducted on magnetic actuators and magnetic effects. Vibration suppression is considered key in civil engineering to ensure the safety and comfort of their occupants and users of mechanical structures. To reduce the system vibration, an effective vibration control with isolation is necessary. Vibration control techniques have classically been categorized into two areas, passive and active controls. For a long time, efforts were made to make the suspension system work optimally by optimizing its parameters, but due to the intrinsic limitations of a passive suspension system, improvements were effective only in a certain frequency range. Compared with passive suspensions, active suspensions can improve the performance of the suspension system over a wide range of frequencies. Semi-active suspensions were proposed in the early 1970s [1], and can be nearly as effective as active suspensions. When the control system fails, the semiactive suspension can still work under passive conditions. Compared with active and passive suspension systems, the semi-active suspension system combines the advantages of both active and passive suspensions because it provides better performance when compared with passive suspensions and is

economical, safe and does not require either higher-power actuators or a large power supply as active suspensions do [2]. In early semi-active suspension, many researches on variable orifice dampers had been done ([3-4]). With these damper types, regulation on of the damping force can be achieved by adjusting the orifice area in the oil-filled damper, thus changing the resistance to fluid flow, but adjusting the speed is slow because of mechanical motion limitations. Another class of semiactive suspension uses controllable fluids. Two fluids that are viable contenders for development of controllable dampers are: electro-rheological (ER) fluids and magneto-rheological (MR) fluids. Although the discovery of both ER and MR fluids dates back to the late 1940's, researchers have primarily concentrated on ER fluids for civil engineering applications ([5-8]). Recently developed MR fluids appear to be an attractive alternative to ER fluids for use in controllable fluid dampers ([9-12]). MR fluids are smart materials, which typically consist of micron-sized, magnetically polarizable particles dispersed in a carrier medium such as mineral or silicone oil. The particles form chain-like fibrous structures in the presence of a high electric field or a magnetic field. When the electric field strength or the magnetic field strength reaches a certain value, the suspension solidifies and will have high yield stress; conversely, the suspension can be liquefied once more by removal of the electric field or the magnetic field. These materials demonstrate dramatic changes in their rheological behavior in response to a magnetic field ([9]). The process of change is very quick, less than a few milliseconds, and can easily be controlled by small amounts of energy on the order of several watts. Consequently, MR fluid dampers, which utilize the advantages of MR fluids, are semi-active control devices that are capable of generating a force with magnitude sufficient for rapid response in large-scale applications, while requiring only a battery for power ([12]). Additionally, these devices offer highly reliable operations and their performance is relatively insensitive to temperature fluctuations or impurities in the fluid ([9]). As a result, there has been active research and development of MR fluid dampers and their applications ([13-18]).

However, major drawbacks that hinder MR fluid dampers applications are their nonlinear force/displacement and hysteretic force/velocity characteristics. Therefore, one of the challenges involved in creating high performance MR fluid damper in control applications is the development of accurate models that can take full advantage of the unique features of the MR device. Both parametric and nonparametric models have been built by researchers to describe the behavior of MR fluid dampers. The parametric models based on mechanical idealizations have been proposed as the Bingham, Bouc-Wen, phenomenological model, and others [19-26]. The Bingham model [19] represents the dry-friction as a signum function on the damper velocity and may be considered as a simple model for describing the hysteresis characteristic. The Bouc-Wen model uses a differential equation to depict the non-linear hysteresis with moderate complexity and is widely applied in building controls. Once the characteristic parameters of the Bouc-Wen model are determined, the model can obtain the linearity and the smoothness of the transition from the pre-yield to the post-yield region. One of the major problems in the Bouc-Wen model is the accurate determination of its characteristic parameters which is obtained by using optimization or trial error techniques. Consequently, these techniques demand high computational cost to generate the model parameters. Moreover, the fact that each set of constant parameters is valid only for single

vibration conditions makes the Bouc-Wen model inappropriate for varying excitation environments. Therefore, many researches on how to develop a MR fluid damper model for higher accuracy and higher adaptability in estimating the behavior of the damper have been done. Spencer *et al* [21] successfully developed a phenomenological model to improve the model accuracy with an additional internal dynamical variable. Choi and Lee [22] designed a hysteresis damper model based on a polynomial and a curve fitting to predict better the damping force when compared with conventional models. Dominguez *et al* [23, 24] proposed a methodology to find out the characteristic parameter of Bouc-Wen model and then designed a new non-linear model to simulate the behavior of the MR fluid dampers. Kwok *et al* designed a hysteretic model based on a particle swarm optimization [25] or using GA technique [26] to modify the Bonc-Wen model and identify the characteristic parameters of the models. The effectiveness of these models with their identification process was proved through the experimental test data. However, the parametric modeling methods require assumptions as regards the structure of the mechanical model that simulates behavior. The approach could be divergent if the initial assumptions for the model structure are flawed, or if the proper constraints are not applied to the parameters. Unrealistic parameters such as negative mass or stiffness may be obtained. Meanwhile, non-parametric methods could avoid these drawbacks of the parametric approaches for modeling, which are adaptive and applicable to linear, nonlinear, and hysteretic systems. For modeling MR fluid dampers, Chang and Roschke [27] proposed a non-parametric model using multilayer perceptron neural network with optimization method for a satisfactory representation of a damper behavior. Schurter and Roschke [28] investigated the modeling of MR fluid dampers with an adaptive neuro-fuzzy inference system. The fuzzy structure was simple for modeling; nevertheless, the training model process relied on input and output information on MR fluid dampers and took much computation time. Wang and Liao [29, 30] explored the modeling of MR fluid dampers by using a trained direct identification based on recurrent neural network. Although, the designed models could predict the dynamic responses of the dampers with high precision, the model architectures and the training methods were complex.

For these reasons, a novel direct modeling method to model simply MR fluid dampers is proposed in this paper. This method uses a self tuning fuzzy (STF) system based on neural technique and was designed to overcome the disadvantages of conventional models. Here, an alternative MR fluid damper model built in the form of the simple fuzzy mapping laws, which use triangle membership functions (MFs) and centreaverage defuzzification, is considered to estimate directly the MR damping force output with respect to the MR characteristics. In order to improve the accuracy of the proposed STF model, the back propagation learning rules based on gradient descent method is used to adjust online the fuzzy parameters to minimize the model error function. Input information for the fuzzy training process is the current supplied for the MR fluid damper and its dynamic responses. Effectiveness of the proposed MR fluid damper modelling method is clearly verified through comparisons of the experimental data obtained from a damper test rig, and modeling results. The results show that the proposed fuzzy interference system trained online by using neural technique has satisfactorily representative ability for the behavior of MR fluid damper with small computational requirement.

The remainder of this paper is organized as follows. Section 2 describes the test rig using a MR fluid damper. In section 3, some common used models are analysed and then the procedure of designing the proposed modeling method is presented. Section 4 shows the modeling results of the MR fluid damper using the proposed STF model. Concluding remarks are presented in section 5.

2. Experimental Apparatus

To take full advantage of the unique features of the MR fluid damper in control applications, a model must be developed that can accurately reproduce the behavior of MR fluid damper. To verify the precision of the proposed modeling method for a MR fluid damper, a test rig using a specific damper was set up to obtain experimental data used in the modelling process and to make a comparison between the real damping response and the MR model output. A MR fluid damper of the RD-1005-3 series manufactured by LORD Corporation was used in this study. The details of the test system are described below.

2.1 MR fluid damper

MR fluid damper is a damper containing special fluid, MR fluid, which is allowed to change its viscosity with respect to an applied external magnetic field. Here, the MR fluid is non-magnetic fluids, such as mineral or silicon oil, carrying tiny magnetic particles, such as carbonyl iron. The fluid is housed within a cylinder and flows through a small orifice. A magnetic coil is built in the piston or on the housing. When a current is supplied to the coil, the particles are aligned and the fluid changes from the liquid state to the semi-solid state within milliseconds. Consequently, a controllable damping force is produced. The force procedure by a linear MR fluid damper depends on magnetic field induced by the current in the damper coil and the piston velocity as in Fig. 1. The damper operates in the flow mode and this means that the produced force is controlled by the flow resistance of the MR fluid portion contained in the gap inside the piston.

The MR fluid damper RD-1005-3 used in this research is a compact magneto-rheological fluid damper unsurpassed in its combination of controllability, responsiveness and energy density. As a magnetic field is applied to the MR fluid inside the mono-tube housing, the damping characteristics of the fluid increase with practically infinite precision. This damper can be adapted to a wide variety of applications because of its simple design, small size, quiet operation, and compact shock absorption with low voltage and current demands that allow for real-time damping control. The photographs and specifications of the damper are displayed in Fig. 2 and Table 1.

Based on the dimensions and characteristics of the damper RD-1005-3, the rig to perform the damping test and to model the damper was designed and set-up as followings.

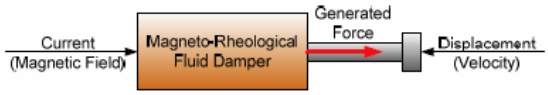

Fig. 1. Diagram of a MR fluid damper

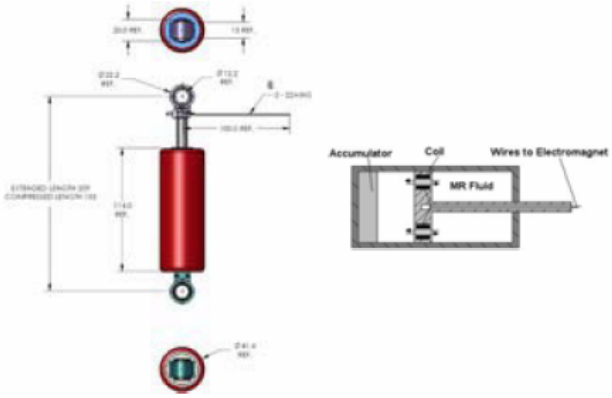

Fig. 2. MR fluid damper RD-1005-3

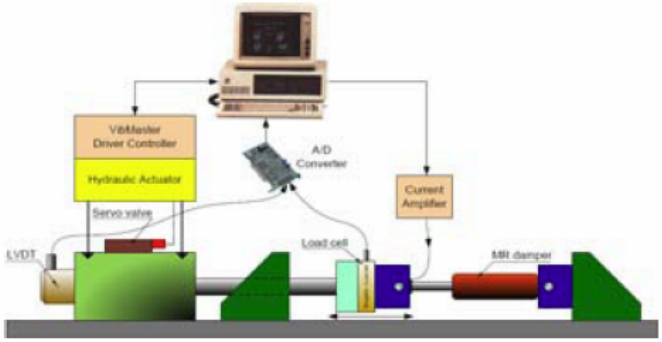

Fig. 3. Diagram of the experimental setup

Table 1 Technical data for the MR fluid damper RD1005-3

Lord MR Fluid damper-RD-1005-3 Series	
Parameter	Value
Compressed length (mm)	155
Extended length (mm)	208
Weight (g)	800
Megneto_Rheological fluid viscosity (pa-s) @ 40^0C Density (g/cm^3) Solid content by weight,% Operating temperature (^{0}C)	MRF-132DG 0.092±0.015 2.98-3.18 80.98 -40 to +130
Electrical Characteristics: Maximum input current (A) Input Voltage (VDC)	 2 12
Mechanical Characteristics: Maximum Extension Force (N) Maximum Operating temperature (^{0}C)	 4448 171
Response time (ms) (amplifier & power supply dependent)	<25 (time to reach 90% of max level during a 0 to1 amp step input)

2.2 Test rig

The schematic diagram of the test rig for the RD- 1005-3 damper is depicted in Fig. 3. In the experimental system, a hydraulic actuator and a driving controller (VibMaster) manufactured by Park electronics were employed to drive the damper. The data acquisition system consisted of up to eight control axes (synchro or individual), up to four analog input channel users, and four analog output channel users. In the actuator, the servo valve with a nominal operational frequency range of 0-50 Hz, made by Moog Inc., was used as the final control target to adjust the motion. The actuator has a 3.5 cm diameter cylinder and a ±20 mm stroke which was fitted with low friction Teflon seals to reduce non-linear effects. A linear variable differential transformer (LVDT) was set-up to measure the displacement of the piston-rod of the MR fluid damper. In addition, a compatible load cell with 500 kgf capacity by Bongshin was attached in series with the damper rod to measure the damping force. A PC installed with the VibMaster control program was used to generate system vibrations, while the PC with a current amplified circuit sent the current signal to adjust the damper characteristic. Consequently, the feedback signals measured by the LVDT and the load cell were sent back to the PC through an Advantech A/D PCI card 1711 to perform full data acquisition with input and output signals.

Finally, the load frame shown in Fig. 3 was designed and fabricated as shown in Fig. 4 for the purpose of obtaining the MR fluid damper response.

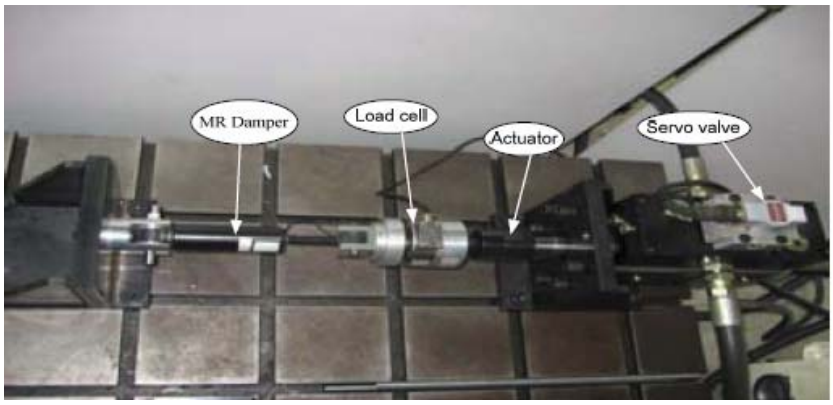

Fig. 4. RD-1005-3 damper in the test rig

3. Modeling of the MR fluid damper with the STF mechanism

Firstly, some common models used to estimate the behavior of a MR fluid damper are revised. Based on the analysis those models, the proposed STF model and its designing process are described in details. The experimental data obtained from the testing system is used for model analyses and designs.

3.1 Experimental systems

To obtain the data used to characterize the RD- 1005-3 MR fluid damper behavior, a series of experiments was conducted under various sinusoidal displacement excitations while simultaneously altering the magnetic coil in a varying current range. The out put of each test

was the force generated by the damper. The system was excited up to ±5mm by the hydraulic actuator within the frequency range of 1 to 2.5Hz. Likewise, the range of current supplied to the coil inside the damper varied from 0 to 1.5A. A sampling time of 0.002 seconds was used to produce 5000 sets of data from the experiments. The parameters for the experiments are listed in Table 2. During all the experiments, the damping force responses were measured together with the variation of piston displacement and supplied current for the damper. Fig. 5 depicts an example of relationship between the piston velocity, the applied current and the dynamic response of the damper in 3D map with respect to 1Hz sinusoidal excitation and 5mm of amplitude applied to the damper.

Table 2 Parameters setting for the experiments on the MR fluid damper test rig

Test No.	Displacement – Sine wave		MR fluid damper current (A)
	Amplitude (mm)	Frequency (Hz)	
01 to 06	± 5	1.0	(0,0.5, 0.75, 1.0, 1.25, 1.5)
07 to 12	± 5	1.5	(0,0.5, 0.75, 1.0, 1.25, 1.5)
13 to 18	± 5	2.0	(0,0.5, 0.75, 1.0, 1.25, 1.5)
19 to 24	± 5	2.5	(0,0.5, 0.75, 1.0, 1.25, 1.5)

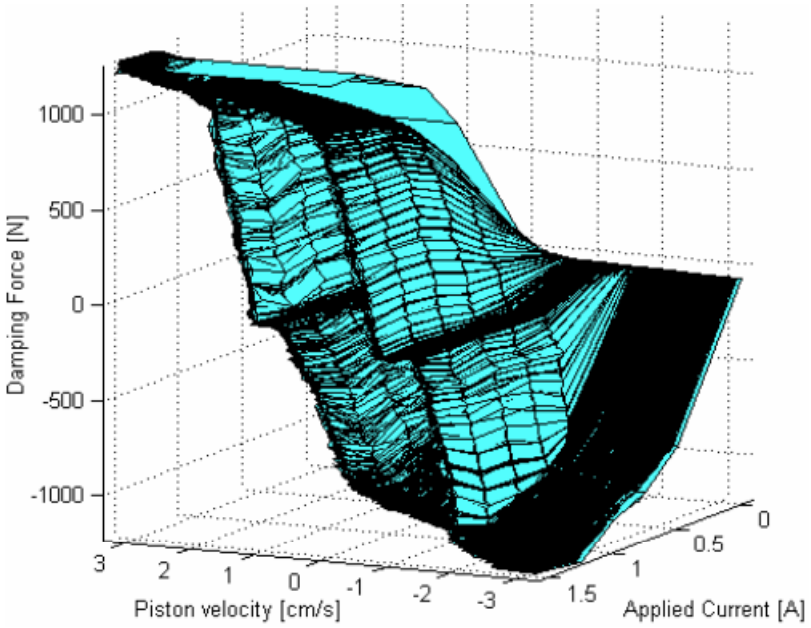

Fig.5: Performance curves for the RD-1005-3 MR fluid damper for a sinusoidal excitation at frequency 1Hz and amplitude 5mm

3.2 Common MR fluid damper models

3.2.1 Bingham model

The stress-strain behavior of the Bingham viscoplastic model [31] is often used to describe the behaviour of MR fluid. In this model, the plastic viscosity is defined as slop of the measured shear stress versus shear strain rate data. Thus, for positive values of the shear rate, $\dot{\gamma}$ the total stress is given by:

$$\tau = \tau_{y(field)} + \eta\dot{\gamma} \qquad (1)$$

Where $\tau_{y(field)}$is the yield stress induced by the magnetic field and η is the viscosity of the fluid.
Based on this model, an idealized mechanical model referred to as the Bingham model was proposed to estimate the behavior of an MR fluid damper by Standway *et al* [19]. This model consists of a Coulomb friction element placed in parallel with a viscous damper as depicted in Fig. 6.

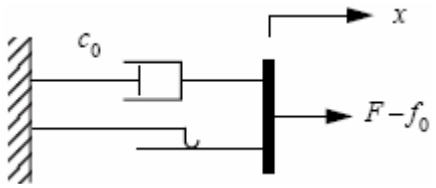

Fig.6: Bingham model of a MR fluid damper

Here, for nonzero piston velocities, $\dot{x}$ the force *F* generated by the device is given by:

$$F = f_c sign(\dot{x}) + C_0\dot{x} + f_0 \qquad (2)$$

where C_0 is the damping coefficient; f_c is the frictional force related to the fluid yield stress; and an offset in the force f_0 is included to account for the nonzero mean observed in the measured force due to the presence of the accumulator. Note that if at any point the velocity of the piston is zero, the force generated in the frictional element is equal to the applied force.

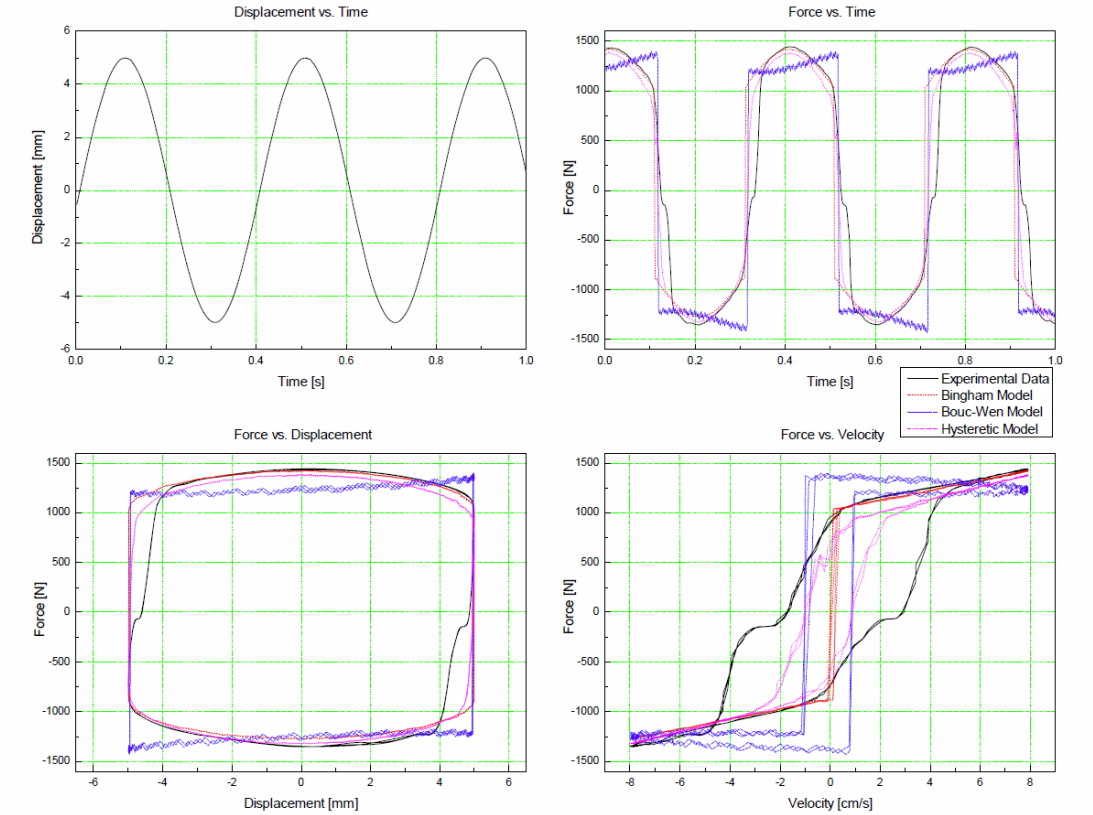

Fig.7: Comparison between experimental data and the predicted damping forces for a 2.5Hz sinusoidal excitation with amplitude 5mm while current supplied to the damper is 1.5A.

To present the damper behavior, the characteristic parameters of the Bingham model in equation (2) need to be chosen to fit with the experimental data of the damping system. For example, those parameters are chosen as C_0 = 50Ns/cm; f_c = 950N and f_0 = 75N for a 2.5Hz sinusoidal excitation with amplitude 5mm while the current supplied to the damper is 1.5A. Consequently, the predicted damping force by using the Bingham model is compared with the experimental response as plotted in Fig. 7 where the predicted and the measured data are the 'dash' and the 'solid line', respectively.

From the results, although the force-time and force-displacement behavior are reasonably modeled, the predicted force-velocity relation is not captured, especially for velocities that are near zero. By using this model, the relationship between the force and velocity is one-to-one, but the experimentally obtained data is not one-to-one. Furthermore, at zero velocity, the measured force has a positive value when the acceleration is negative (for positive displacements), and a negative value when the acceleration is positive (for negative displacements). This behavior must be captured in a mathematical model to adequately characterize the device. Hence, Gamota and Filisko [20] developed an extension of the Bingham model, which is given by the viscoelastic-plastic model shown in Fig. 8.

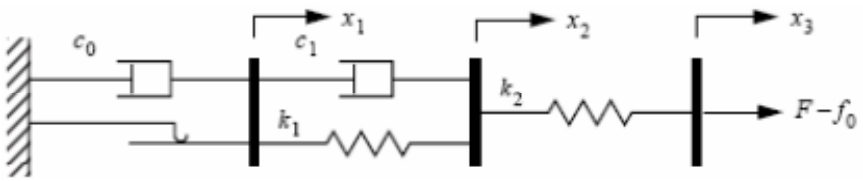

Fig.8: Extended Bingham model of a MR fluid damper

The model consists of the Bingham model in series with a standard model. The governing equations for this model are given as followings

$$\left.\begin{aligned} F &= k_1(x_2 - x_1) + c_1(\dot{x}_2 - \dot{x}_1) + f_0 \\ &= c_0\dot{x}_1 + f_c \operatorname{sign}(\dot{x}_1) + f_0 \\ &= k_2(x_3 - x_2) + f_0 \end{aligned}\right\}, \quad |F| > f_c \quad (3)$$

$$\left.\begin{aligned} F &= k_1(x_2 - x_1) + c_1\dot{x}_2 + f_0 \\ &= k_2(x_3 - x_2) + f_0 \end{aligned}\right\}, \quad |F| \le f_c \quad (4)$$

Where C_0 is the damping coefficient associated with the Bingham model; k_1, k_2 and C_1 are associated with the linear solid material. This model can present the force-displacement behaviour of the damper better the Bingham model. However, the governing equations (3), (4) are extremely stiff, making them difficult to deal with numerically [21]. Therefore, the Bingham model or extended Bingham model are normally employed in case there is a significant need for a simple model.

3.2.2 Bouc-Wen model

One model that is numerically tractable and has been used extensively for modeling hysteretic systems is the Bouc-Wen model. This model contains components from a viscous damper, spring and a hysteretic component. The model can be described by the force equation and the associated hysteretic variable as given

$$F = c\dot{x} + kx + \alpha z + f_0 \quad (5)$$

$$\dot{z} = -\gamma|\dot{x}|z|z|^{n-1} - \beta\dot{x}|z|^n + \delta\dot{x} \quad (6)$$

where: F is the damping force; f_0 is the offset force; c is the viscous coefficient; k is the stiffness, $\dot{x}$ and x are the damper velocity and displacement; α is a scaling factor; z is the hysteretic variable; and γ , β , δ ,n are the model parameters to be identified. Note that when $\alpha = 0$, the model represents a conventional damper.

In order to determine the Bouc-Wen characteristic parameters predicting the MR fluid damper hysteretic response, Kwok *et al* [26] proposed the nonsymmetrical Bouc-Wen model with following modifications

$$F = c\left(\dot{x} - \mu\operatorname{sign}(z)\right) + kx + \alpha z + f_0 \quad (7)$$

$$\dot{z} = \left\{-\left[\gamma\operatorname{sign}(z\dot{x}) + \beta\right]|z|^n + \delta\right\}\dot{x} \quad (8)$$

Where μ is the scale factor for the adjustment of the velocity.

As the optimization results for the test rig applied the damper RD-1005-3 by using GA in [23], the relationships between the Bouc-wen parameters and the supplied magnetization current, i, are given as

$$
\begin{aligned}
&c = 2.65\times10^{3}i + 2.05\times10^{3};\\
&k = 1.99\times10^{3}i + 5.57\times10^{3};\\
&\alpha = 2.11\times10^{3}i + 1.68\times10^{3}\\
&f_0 = 0.6i - 12.43; \mu = -0.02i + 1.25;\\
&n = 0.12i + 1.58\\
&\delta = 0.5\times10^{5}i + 2.5\times10^{5};\\
&\beta = -0.45\times10^{6}i + 3.18\times10^{6};\\
&\gamma = 0.39\times10^{6}i + 3.6\times10^{6}
\end{aligned}
\qquad (9)
$$

The Bouc-Wen model built from equations from 7 to 9 is tested for modeling the damping force in this study. As a result, the predicted force is plotted as the 'dash-dot' line in Fig. 7 for a 2.5Hz sinusoidal excitation with amplitude 5mm while the current supplied to the damper is 1.5A. From the result, it is clearly that to obtain good predicted behavior of a MR fluid damper in a specific system, the Bouc-Wen parameters must be tuned by using optimization or trial error techniques which causes high computational cost to obtain the optimal parameters. Furthermore, to obtain better modeling performance, some modified Bouc-Wen models have been proposed. The research results in [21] show that the modified Bouc-Wen model improves the modeling accuracy. However, the model complexity is unavoidably increased with an extended number of model parameters (14 parameters need to be identified in [21]) which may impose difficulties in their identification and take much time for optimization process [28].

3.2.3 A hysteretic model

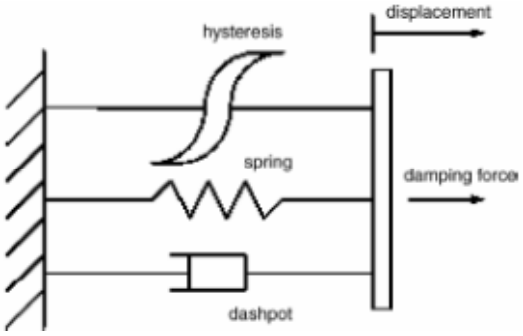

Fig.9: Hysteretic model of a MR fluid damper

For a simple model, Kwok *et at* [25] proposed a hysteretic model to predict the damping force of the MR fluid damper RD-1005-3 as illustrated in Fig. 9. The model can be expressed as following equations

$$F = c\dot{x} + kx + \alpha z + f_0 \qquad (10)$$

$$z = \tanh\left(\beta\dot{x} + \delta sign(x)\right) \qquad (11)$$

where: c and k are the viscous and stiffness coefficients; α the scale factor of the hysteresis; z the hysteretic variable given by the hyperbolic tangent function and f_0 is the damper force offset; and β , δ are the model parameters to be identified.

As the results in [25], the parameters in equations 9 and 10 are given:

$$C = 1929i + 1232; k = -1700i + 5100;$$

$$\alpha = -244i^2 + 918i + 32;\ f_0 = -18i + 57 \qquad (12)$$

$$\beta = 100;\ \delta = 0.3i + 0.58$$

However, to obtain the parameters as in equation (12), a swam optimization [26] based on GA algorithm must be used to select the most suitable values with respect to each specific system using the damper RD-1005-3. Hence, when using the set of resulting parameters in [26] to apply to the test system of the MR fluid damper RD-1005-3 in this study, the hysteretic model cannot present well the damper behavior. For example, the modeling result by using the hysteretic model, for a 2.5Hz sinusoidal excitation with amplitude 5mm while the current supplied to the damper is 1.5A, is depicted in Fig. 7 as the 'short dash' line. The result proves that although the estimated force in this case is better than in case of using Bingham or Bouc-Wen model, the nonlinear characteristic of the damper cannot be described well. Moreover, the swam optimization is also take training time to generate the parameters of hysteretic model.

3.3 Proposed MR fluid damper model based on STF

From above analyses, the common models can predict the characteristic of a MR fluid damper with high accuracy and applicability. However, the parameters representing those models need to be tuned by using optimization or trial error techniques which causes high computational cost to generate the parameters. In addition, those models only adapt with specific damping systems. For a new system, the optimization process must be done again for a full prediction the damper behavior. Therefore, a non-parametric method based on intelligent techniques, for example, is an effective solution to estimate directly the MR fluid damper behavior with high precision.

Fuzzy system is an intelligent tool imitating the logical thinking of human and then is capable of approximating any continuous function. However, there is no systematic method to design and examine the number of rules, input space partitions and membership functions (MFs). Meanwhile, neural network mimics the biological information processing mechanisms. It is typically designed to perform a nonlinear mapping from a set of inputs to a set of outputs. They are non-programmed adaptive information processing systems that can autonomously develop operational capabilities in response to an information environment. It learns from experience and generalizes from previous examples. This technique modifies its behavior in response to the environment, and is ideal in case that the required mapping algorithm is un-known and the tolerance to faulty input information is required. Hence an identification system using fuzzy and neural theory can easily be selected as an effective method for directly modeling MR fluid dampers purpose.

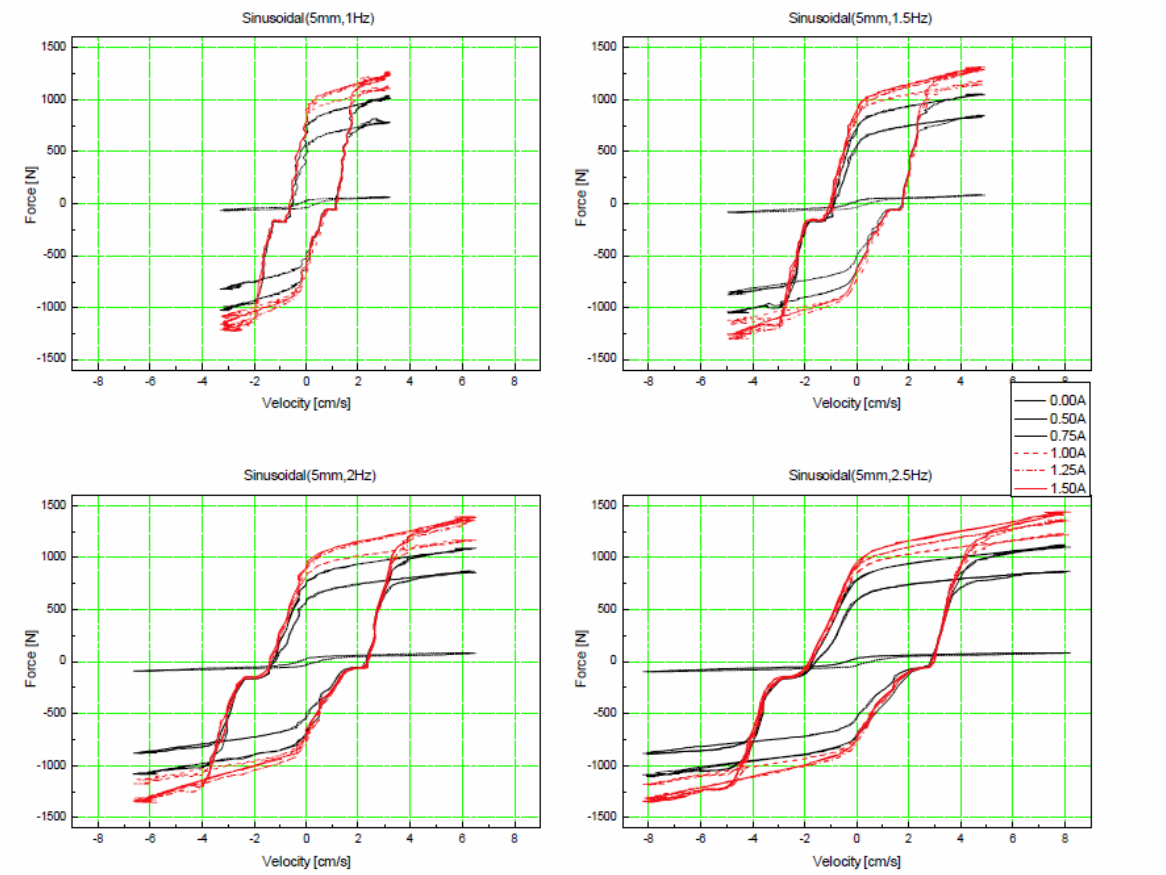

Fig.10: Experimental data measured at sinusoidal excitations (frequency range (1, 2.5) Hz and 5mm of amplitude), and supplied current in range (0, 1.5) A

Here, a newly simple direct modeling method for a MR fluid damper based on the STF mechanism is proposed. This proposed model is based on centreaverage defuzzification architecture, which is a computationally efficient and well suited for implementation of non linear system. In addition, the back propagation is used to decide online the shapes of membership function and fuzzy rules together with the gradient descent method to minimize the modelling error. As a result, the designed fuzzy inference system has higher learning ability that improves the identification quality. The following analyses are used to design the proposed STF model.

The fist factor affecting the dynamic response of the damper is the applied displacement on the piston rod. Fig. 10 displaces the comparison between damping results under various sine excitations with 5mm amplitude and frequency range from 1Hz to 2.5Hz while the supplied current level is in range from 0 to 1.5A. The results show that at fixed current level applied to the damper, the damping force varies due to the piston rod velocity which is caused by the simultaneous change of frequency and/or amplitude of the applied excitation.

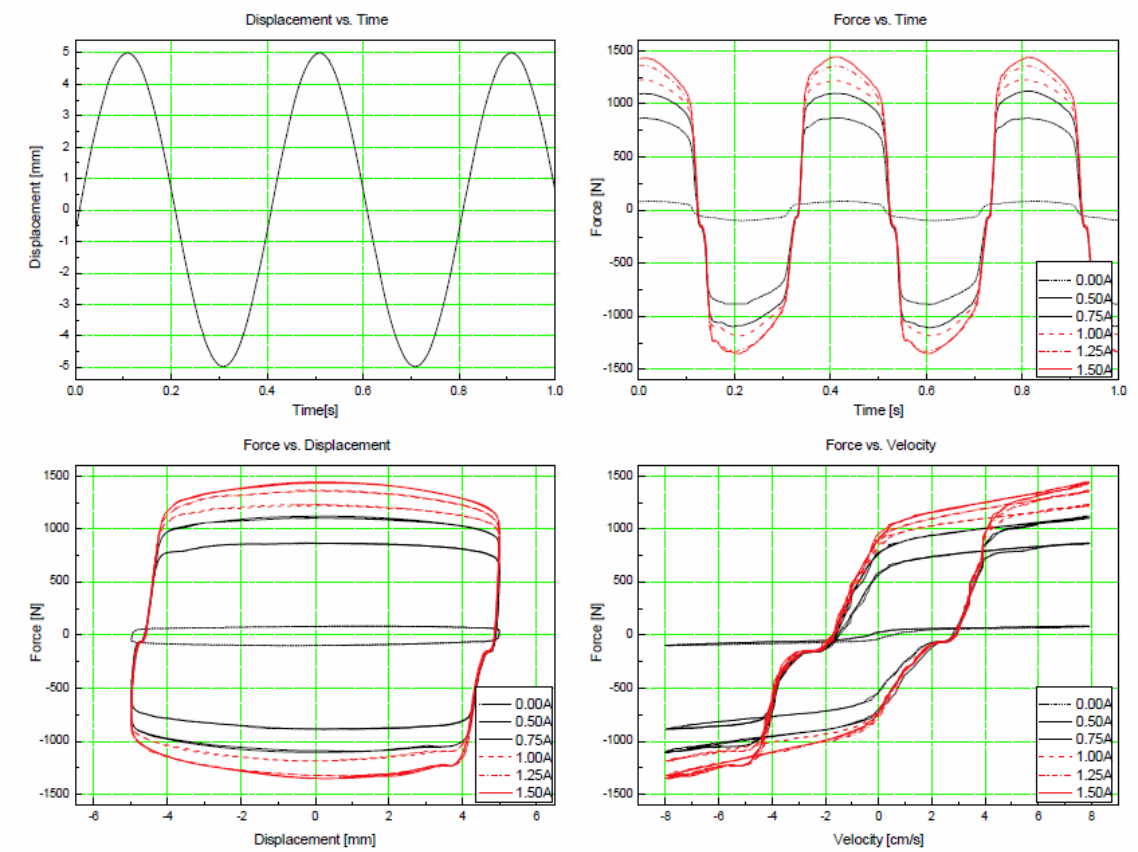

Fig.11: Experimental data measured at sinusoidal excitation (frequency 2.5Hz, and amplitude 5mm), and within current range (0.5, 1.5) A

The second factor affecting the behavior of the damper is the changing of current applied to the damper coil. Fig. 11 shows an example of measuring results in plots of force-time, force-displacement, and force-velocity relation with respect to a 2.5Hz sinusoidal excitation and 5mm of amplitude while the current supplied to the damper is in range between 0 and 1.5A. From this figure, it is readily apparent that as follows:

- The force produced by the damper is not centered at zero. This effect is due to the effect of an accumulator containing high pressure nitrogen gas in the damper. The accumulator helps to prevent cavitations in the fluid during normal operation and accounts for the volume of fluid displayed by the piston rod as well as thermal expansion of the fluid.
- The greater current level, the greater damping force.
- The force increasing speed is faster at lower current levels because of the effect of magnetic field saturation.

Based on the above analyses, the damping force of the MR fluid damper depends on the displacement/ velocity of the damper rod and the current supplied for the coil inside the damper. Therefore, the designed STF model contains two parts: one is the neural-fuzzy inference (NFI) that is used to estimate the damping force (u) caused by the displacement of the damper rod, and the other is the scheduling gain fuzzy inference (SGFI) which is used to switch between the damping force levels (k) with respect to the current levels supplied for the MR coil. Consequently, the estimated damping force of the STF model (f_{MR_est}) is computed as a multiple of the NFI estimated force and the SGFI gain

$$f_{MR\_est} = k \times u \qquad (13)$$

To evaluate the accuracy of the MR model, an error function (E) is defined by the difference between the damping force (f_{MR_est}) estimated from the MR model and the real damping force obtained from experiment (f_{MR}) when the input conditions (MR current and displacement/velocity) for both the model and real MR fluid damper system are the same. Therefore, the error function is expressed by the following equation:

$$E = 0.5(f_{MR_{est}} - f_{MR})^2 \qquad (14)$$

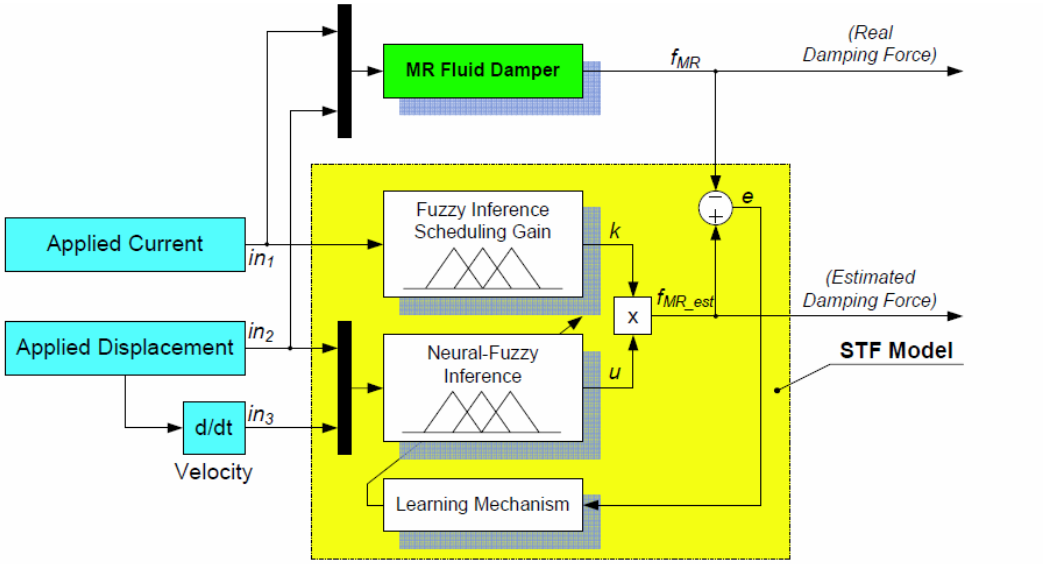

Fig.12: Structure of identification for a MR fluid damper using proposed STF model

Finally, to improve the identification quality of the proposed model, a learning mechanism using neural methodology is used to adjust the fuzzy parameters with the purpose of modeling error minimization. Hence, the overall structure of the proposed STF model for a MR fluid damper is shown in Fig. 12.

3.3.1 Neural-Fuzzy inference (NFI)

The NFI system takes part in estimating the damping force caused by the applied displacement to the damper. The NFI set is therefore designed with two inputs (*in2*, and *in3*) and one output (u).

The ranges of these inputs are from -1 to 1, which are obtained from the applied displacement, and its derivative (velocity) through scale factors chosen from the range of displacement and specification of the MR fluid damper. For each input variable, five triangle membership functions (MFs) are used. Here, "NB", "NS", "ZE", "PS" and "PB" are "Negative Big", "Negative Small", "Zero", "Positive Small" and "Positive Big", respectively. The centroids of the MFs are set initially at the same intervals and the same shape sizes as in Fig. 13a. Because all of the MFs are triangle shapes, so we can express these MFs as follows:

$$\mu(x_i) = \frac{1 - 2|x_i - a_{ji}|}{b_{ji}}, j = 1,2 \dots \dots \dots \dots \dots \dots N \qquad (15)$$

Where a_j is the centre of the j^{th} triangle and b_j is the width; N is the number of triangles.

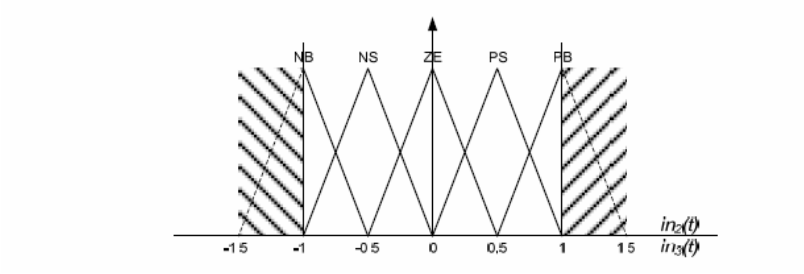

(a) Initial membership functions for NFI inputs: $in_2(t)$, $in_3(t)$

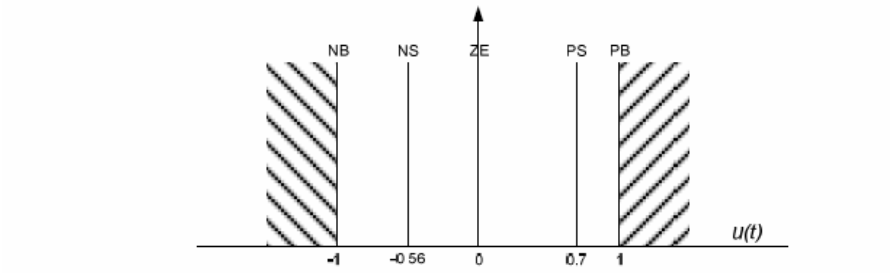

(b) Initial membership functions for NFI output: $u(t)$

Fig.13: Initial Membership functions of the NFI inputs and output

The fuzzy reasoning results of outputs are determined by an aggregation operation of fuzzy sets of inputs and the designed fuzzy rules, where the MAXMIN aggregation method and "centroid" defuzzification method are used. In the proposed neural-fuzzy inference, with a pair of inputs (in_2, in_3), the output of the proposed neural-fuzzy system can be computed as

$$u = \frac{\left(\sum_{j=1}^{M} \mu_j w_j\right)}{\left(\sum_{j=1}^{M} \mu_j\right)} \qquad (16)$$

where μ_j and w_j are the height and weight of the NFI output respectively, which are obtained from the rule j^{th}. The output u of the NFI system has five membership functions: "NB", "NS", "ZE", "PS", and "PB", with the same meaning as the MFs of the inputs. The ranges of the output are set from -1 to 1. The estimated force is then obtained by multiplying the output and a scale factor chosen from the specification of the MR fluid damper. The initial output weights are decided from the experimental results with constant supplied current where the damping force values are caused by the corresponding point of input displacement and velocity. Figure 14 shows an example of these experiments. Here the force value of compression or extension is not the same even if they have the same velocity because of the nonlinearity of the damper. Therefore, the output weights are not set initially at the same intervals as in Fig. 13b.

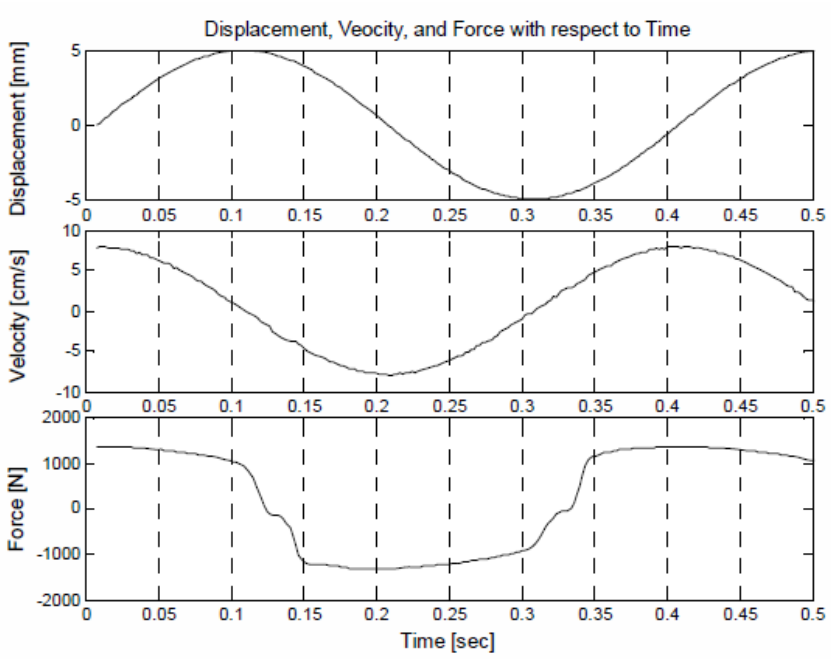

Fig.14: Experimental results: displacement, velocity and force vs. time at a sinusoidal excitation (frequency 2.5Hz and amplitude 5mm)

Table 3 Rules table for neural-fuzzy inference of the STF MR model

Estimated MR force - u		Velocity - in3				
		NB	NS	ZE	PS	PB
Displacement - in2	NB	NB	NB	NM	ZE	PB
	NS	NB	NM	NM	PM	PB
	ZE	NB	NM	ZE	PM	PB
	PS	NB	NM	PM	PM	PB
	PB	NB	ZE	PM	PB	PB

By using the above fuzzy sets of input, output variable, experimental data, damper behaviors, and experiences, the fuzzy rules for the NFI part of the MR model are described in Table 3. Five membership functions for the each input are used to decide the total twenty five rules by using an IF-THEN structure. Here, one fuzzy rule is composed as follows:

Rule *i*: IF displacement (in_2) is *Ai* and velocity (in_3) is *Bi* THEN MR force (u) is *Ci* (i=1,2, .., 25) where *Ai*, *Bi*, and *Ci* are the i^{th} fuzzy sets of the input and output variables used in the fuzzy rules. *Ai*, *Bi*, and *Ci* are also the linguistic variable values in_2, in_3, and u, respectively. Furthermore, the NFI system is online optimized by using the neural network as mention above. The idea of the proposed method is to use a back propagation algorithm to tune the input membership functions shape and the weight of the NFI output during the system operation process to minimize the modelling error. The decisive factors in the inputs MFs *aj*, *bj*, and the weights of the outputs *wj* are automatically updated by using the neuron network. The following set of equations shows the back propagation algorithm:

$$
\begin{aligned}
a_{i(i+1)} &= a_{ji} - \eta_a \frac{\partial E}{\partial a_{ji}} \\
b_{j(i+1)=b_{ji}} &- \eta_b \frac{\partial E}{\partial b_{ji}} \\
w_{j(i+1)=w_{ji}} &- \eta_w \frac{\partial E}{\partial w_{ji}}
\end{aligned} \tag{17}
$$

Where, η_a, η_b and η_w are the learning rate which determine the speed of learning; E is the error function defined by (14).

The factor $\frac{\partial E}{\partial w_{ji}}$ in equation (17) can be calculated as

$$
\frac{\partial E}{\partial w_{ji}} = \frac{\partial E}{\partial f_{MR\_est}} \frac{\partial f_{MR\_est}}{\partial u} \frac{\partial u}{\partial w_i} \tag{18}
$$

Where

$$
\frac{\partial E}{\partial f_{MR\_est}} = e(t) = f_{MR\_est}(t) - f_{MR}(t) \tag{19}
$$

$$
\frac{\partial f_{MR\_est}}{\partial u} = k \tag{20}
$$

$$
\frac{\partial u}{\partial w_i} = \frac{\mu_i}{\left(\sum_{j=1}^{M} \mu_j\right)_i} \tag{21}
$$

The next factors $\frac{\partial E}{\partial a_{ji}}$ in (17) can be computed by:

$$
\frac{\partial E}{\partial a_i} = \frac{\partial E}{\partial f_{MR\_est}} \frac{\partial f_{MR\_est}}{\partial u} \frac{\partial u}{\partial \mu_i} \frac{\partial \mu_i}{\partial a_i} \tag{22}
$$

Where: and $\frac{\delta E}{\delta f_{MR\_est}}$ are $\frac{\partial f_{MR\_est}}{\partial u}$ calculated by using (19) and (20), respectively.

$$
\frac{\partial u}{\partial \mu_i} = \frac{\sum_{j=1}^{M} \mu_j (w_i - w_j)}{\left(\sum_{j=1}^{M} \mu_j\right)^2} \tag{23}
$$

$$
\frac{\partial \mu_i}{\partial a_i} = sign(x - a_i) \frac{2}{b_i} \tag{24}
$$

The final factor $\frac{\partial E}{\partial b_{ji}}$ in (17) can be found by:

$$\frac{\partial E}{\partial b_i} = \frac{\partial E}{df_{MR\_est}} \frac{df_{MR\_est}}{\partial u} \frac{\partial u}{\partial \mu_i} \frac{\partial \mu_i}{\delta b_i} \tag{25}$$

Where: $\frac{\partial E}{df_{MR\_est}}$; $\frac{df_{MR\_est}}{\partial u}$ and $\frac{\partial u}{\partial \mu_i}$ is calculated by using (19), (20), and (23), respectively.

$$\frac{\partial \mu_i}{\delta b_i} = \frac{2|x - a_i|}{b_i^2} \tag{26}$$

With the self learning of neural network technique and the decreasing of the modeling error, the proposed NFI model works more effectively with high accuracy when compared to the real damping response.

3.3.2 Scheduling gain fuzzy inference (SGFI)

This section provides a description of scheduling gain fuzzy inference which works as an intelligent switch to tune the damping force levels (k) with respect to the current levels supplied for the MR coil. The SGFI system is then designed with a single input ($in1$) and a single output (k).

The range of the input is from 0 to 1, which is obtained from the supplied current through a scale factor chosen from the current range for the MR fluid damper coil. Five triangle membership functions, "Z"(Zero), "VS"(Very Small), "S"(Small), "M"(Medium), and "B"(Big), are used for this input variable. The centroids of the MFs are set at the same initial intervals and the same shape sizes as in Fig. 15a. These MFs can then be expressed in the same form as (15).

By using a fuzzy system with the same structure as the NFI system in section 3.3.1, with an input value (in_1), the output gain (k) can be computed as

$$k = \frac{\sum_{q=1}^{Q} \mu_q w_q}{\sum_{q=1}^{Q} \mu_q} \tag{27}$$

Where μ_q and w_q are the height and weight of the SGFI output respectively, which obtained from the rule q^{th}.Table 4 Rules table for scheduling gain inference of the STF MR model

Supplied Current (in_1)	Z	VS	S	M	B
Damping Force - Gain (k)	VS	S	M	B	VB

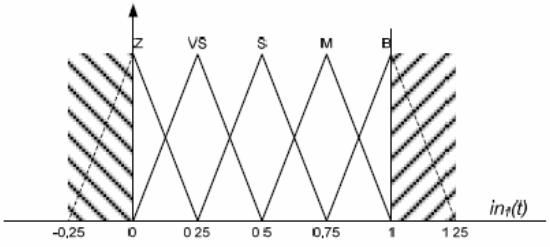

(a) M for SGFI input: $in_1(t)$

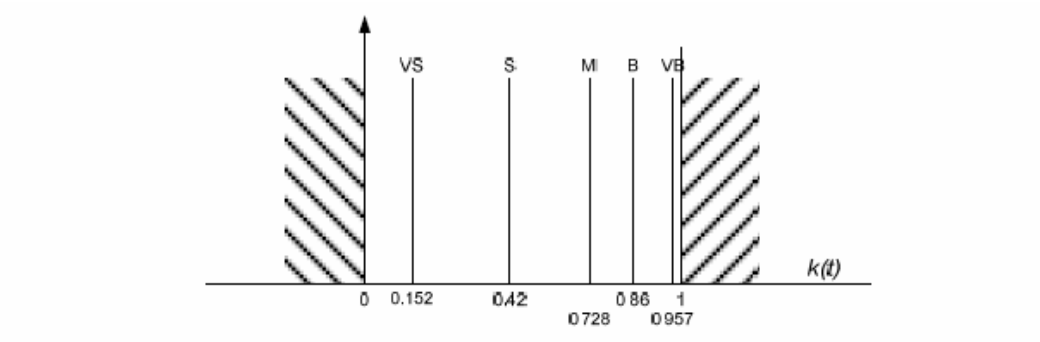

(b) Membership functions for SGFI output: *k(t)*

Fig.15: Membership functions of the SGFI inputs and output

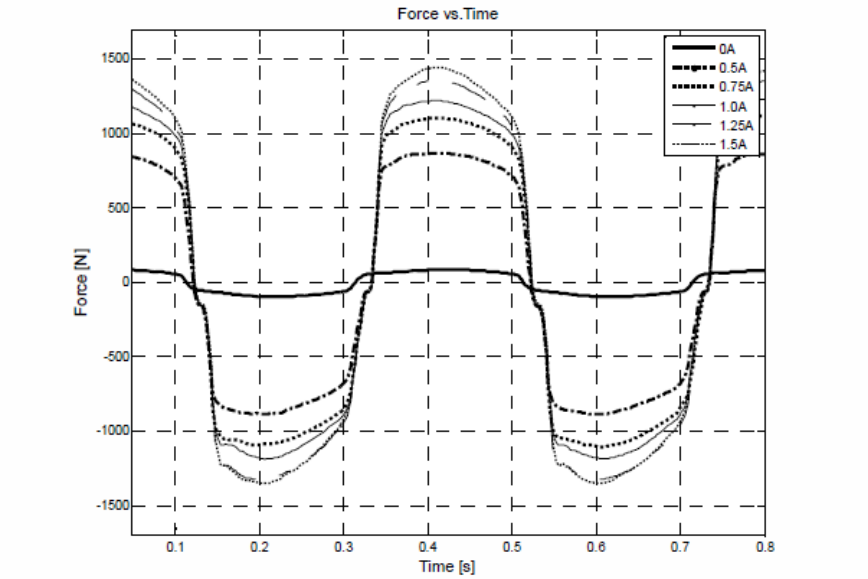

Fig.16: Damping force response in different current levels at a sinusoidal excitation (frequency 2.5Hz and amplitude 5mm)

For the output *k* of the SGFI system, five MFs are used. Here, "VS", "S", "M", "B", and "VB" are "Very Small", "Small", "Medium", "Big", and "Very Big", respectively. The ranges of the output are set from 0 to 1. The output force level is then obtained by multiplying the gain *k* and a scale factor chosen from the specification of the MR fluid damper. The output weights are decided based on the experimental results and the characteristics of the MR fluid damper. Fig. 16 shows examples of experimental results with different current levels supplied to the damper while the generated displacements were the same. Therefore, the output weights are set as in Fig. 15b. By using the above fuzzy sets of input, and output variables, the fuzzy rules for the SGFI part in the MR model are described in Table 4 by using an IF-THEN structure. Finally, the output of the proposed STF MR model (f_{MR_est}) is the multiplication of the NFI output (u) and the SGFI output gain (k) as in equation (13).

4. Modeling results and comparisons

In this section, simulations are carried out to evaluate the ability of the proposed STF model when comparing with the measured dynamic responses. The experimental data including the piston displacement and current supplied for the damper coil will be used as the inputs of the

suggested MR model (section 3.3). Consequently, the model output, damping force, is directly obtained through the fuzzy mapping system. At that time, the parameters of the STF model are updated after each step of simulation time through the online training process by using the neural technique. Here, the deviation between the predicted force and measured force is fed back to the learning mechanism (see Fig. 12) inside the STF model as training target. The STF parameters are continuously adjusted in the direction to minimize the modeling error in equation (14) and then, the proposed STF model can accurately capture the force responses of the MR fluid damper in the varying of working conditions. Firstly, the dynamic responses were measured by doing experiments on the test rig with a various sinusoidal displacement excitations whose frequency is in the range from 1Hz to 2.5Hz, and 5mm amplitude while the applied current for the damper coil is changed from 0A to 1.5A. Figure 17 displays the modeling results of the proposed STF model in a comparison with the real damping behavior for a 2.5Hz sinusoidal displacement. The results show that with the STF modeling method, the nonlinear characteristic of the MR fluid damper can be directly estimated with high accuracy for both the force/time, force/displacement, and force/velocity relation in despite of the varying of applied current for the damper. The STF model shows a good predicting result especially on low current level. When the value of velocity is high, the proposed model describes well the MR fluid damper hysteresis. But in the zero velocity regions, there are some error that is because of the system compliance and the existing noise in experimental environment. To obtain the high modelling precision as shown in Fig. 17, the STF parameters were online optimized by the leaning mechanism with respect to the modeling error cost function. Fig. 18 shows the membership functions of the STF system after training to obtain the better estimated force of the MR fluid damper for a 2.5Hz sinusoidal displacement excitation and 1.5A of the applied current. As the result, the proposed STF model can predict the damping force with higher accuracy.

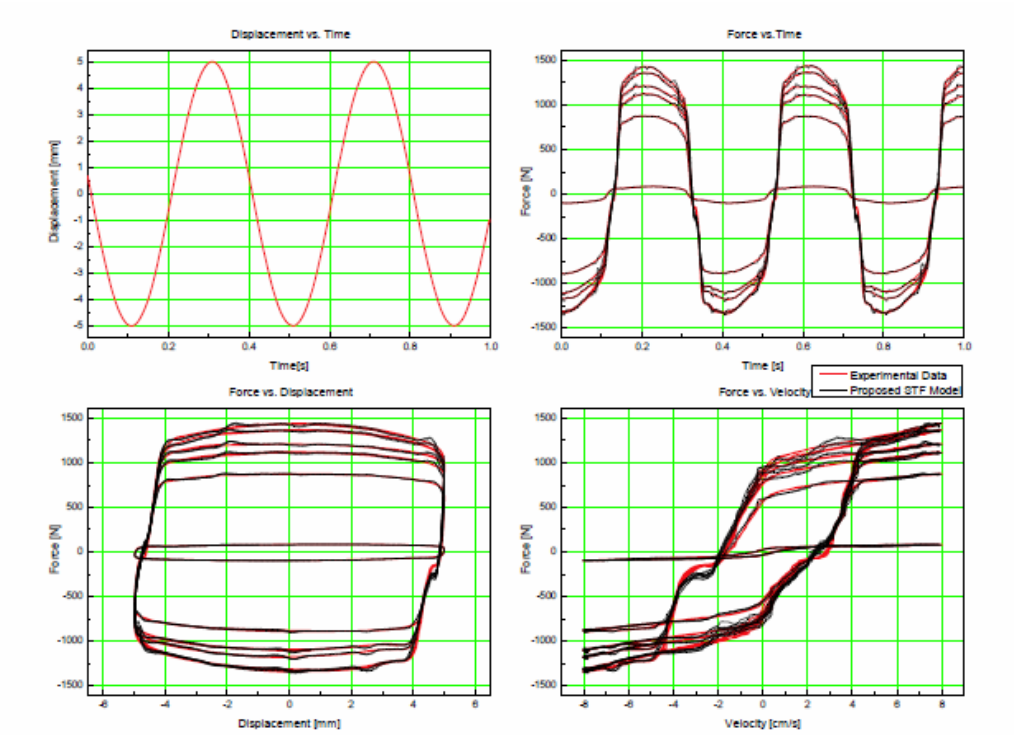

Fig.17: Comparison between the estimated force and actual damping force for an applied current range (0, 1.5) A at a sinusoidal excitation (frequency 2.5Hz and amplitude 5mm)

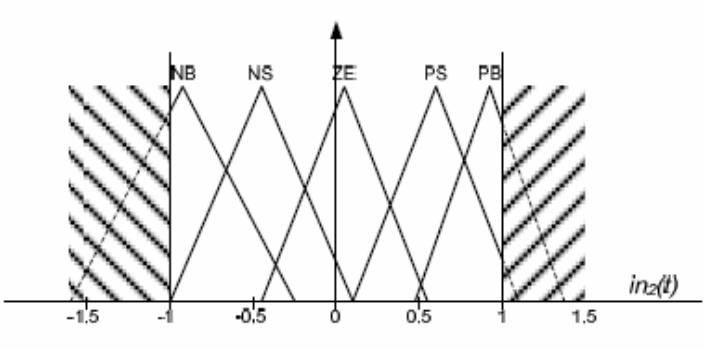

(a) MFs for NFI input $in_2(t)$ after training

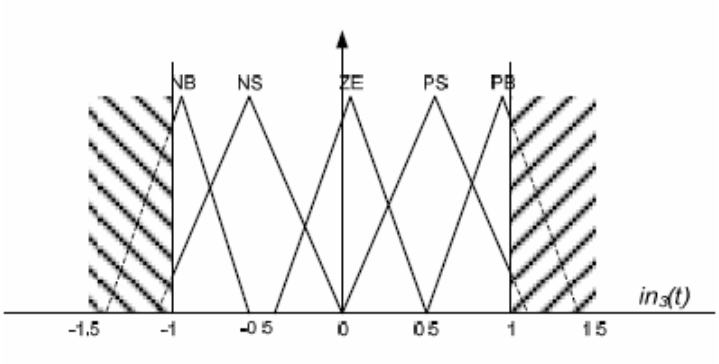

(b) MFs for NFI input $in_3(t)$ after training

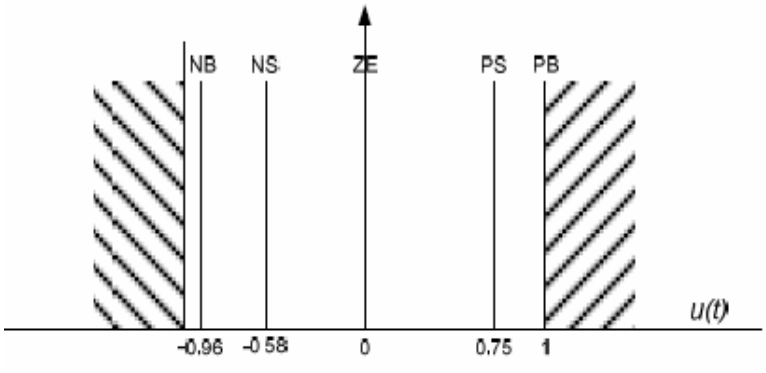

(c) MFs for NFI output $u(t)$after training

Fig.18: MFs of the NFI inputs and output after training

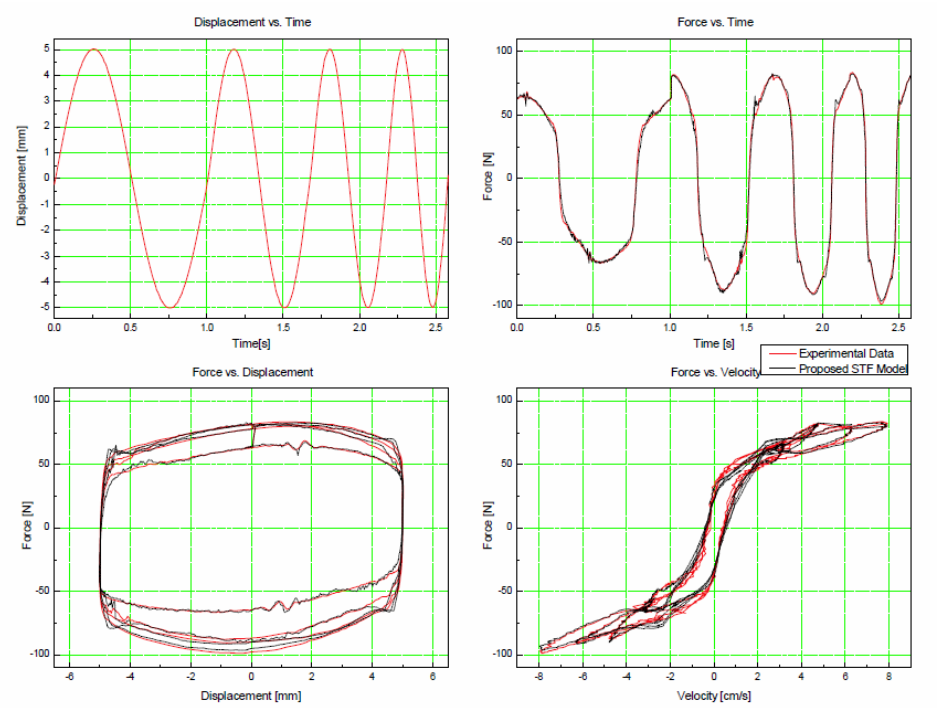

Fig.19: Comparison between the estimated force and actual damping force for an applied current 0A at a chirp excitation (frequency range (1, 2.5) Hz and amplitude 5mm)

Secondly, displacement excitations with a continuous variation of frequency were used to fully check the ability of the designed modeling method in case of varying excitation environments. Since, experimental data were measured from the damping system with the chirp displacement excitations whose frequency was varied from 1Hz to 2.5Hz.

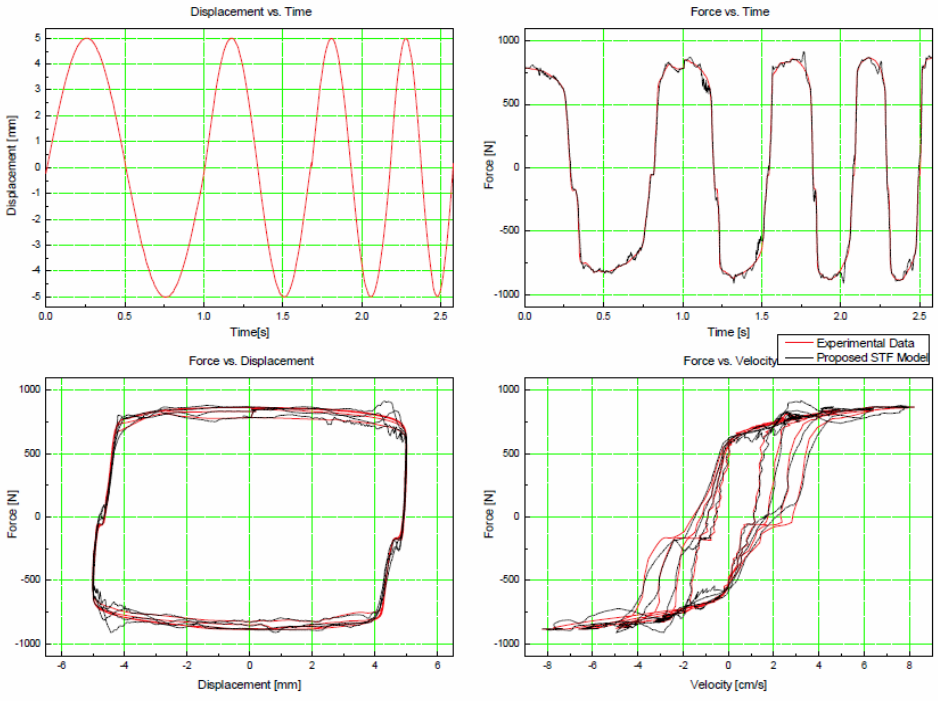

Fig.20: Comparison between the estimated force and actual damping force for an applied current 0.5A at a chirp excitation (frequency range (1, 2.5) Hz and amplitude 5mm)

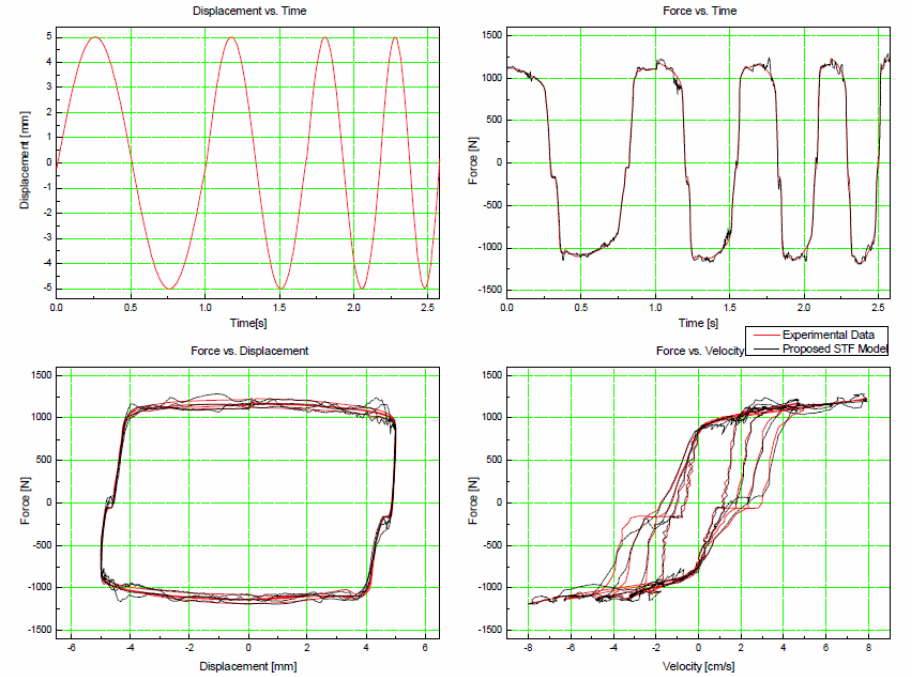

Fig.21: Comparison between the estimated force and actual damping force for an applied current 1.0A at a chirp excitation (frequency range (1, 2.5) Hz and amplitude 5mm)

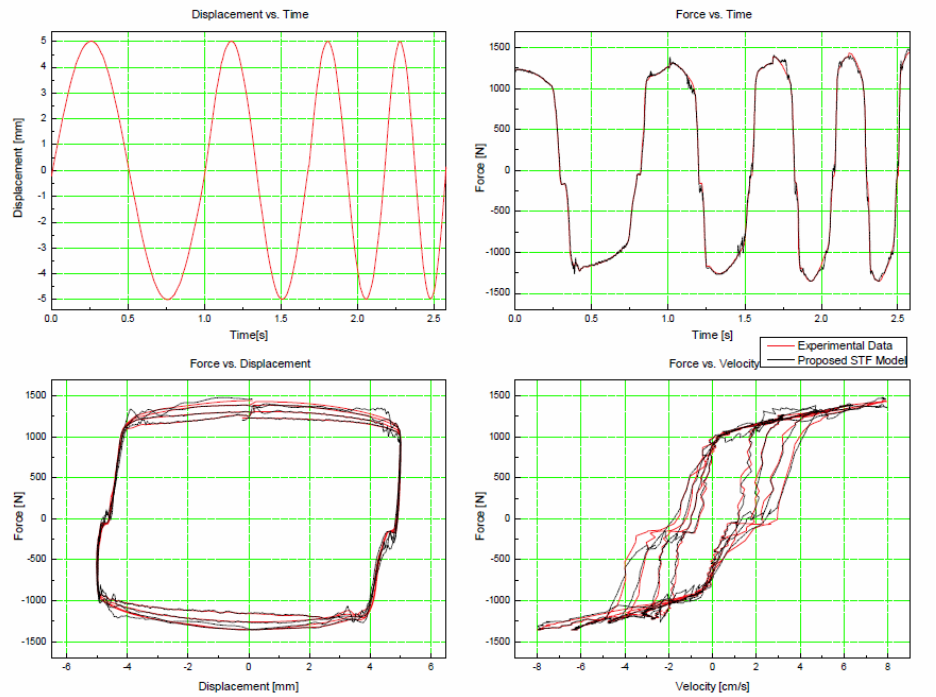

Fig.22: Comparison between the estimated force and actual damping force for an applied current 1.5A at a chirp excitation (frequency range (1, 2.5) Hz and amplitude 5mm)

Figures 19, 20, 21, and 22 depict the comparisons of the real damping responses and the estimated forces in case of 0A, 0.5A, 1A and 1.5A of the applied current for the MR fluid damper coil. From these results, it is clearly that with the online self tuning ability, the proposed model has enough strong to describe well the nonlinear behavior of the damper under various excitation environments, especially in case of low supplied current level.

5. Conclusion

In this paper, a simple direct modeling method for a MR fluid damper using the STF mechanism is proposed. Furthermore, a test rig using the MR fluid damper was fabricated to verify the effectiveness of the suggested model. Based on the experimental results and modeling results, it is clear that the STF model can predict the force-displacement behavior of the MR damper well with high precision. In addition, the proposed STF model with the online self tuning ability based on the neural technique does not require computational time to generate the characteristic parameters of the model as the common used modelling methods such as Bouc-Wen model. Consequently, the STF model can automatically adjust its parameters to adapt to a damping system containing large nonlinearities and a working environment under perturbation. Based on the proposed model, a controller can be easier designed to control the suspension system with high performance.

Acknowledgement

This work was supported by Brain Korea 21 (BK21). The authors would like to acknowledge the significant contributions provided by Brain Korea 21 (BK21).

References

[1] D. Karnopp, M. J. Crosby, and R. A. Farwood, Vibration control using semi-active force generators, *ASME J. Eng. Ind.*, 96(2), (1974) 619-626.

[2] K. Yi, and B. S. Song, A new adaptive sky-hook control of vehicle semi-active suspensions, *Proc. Of I Mech E Part D J. of Auto. Eng.*, 213(3), (1999) 293-303.

[3] K. Kawashima, S. Unjoh, and K. Shimizu, Experiments on Dynamics Characteristics of Variable Damper, Proc. of the Japan National Symp. On Structural Response Control, Tokyo, Japan, (1992) 121.

[4] T. Mizuno, T. Kobori, J. Hirai, Y. Matsunaga, and N. Niwa, Development of Adjustable Hydraulic Dampers for Seismic Response Control of Large Structure, ASME PVP Conf., (1992) 163-170.

[5] H. P. Gavin, Y. D. Hose, and R. D. Hanson, Design and Control of Electrorheological Dampers, Proc. of the First World Conf. on Structural Control, Pasadena, CA, (1994) 83-92.

[6] W. C. Park , S. B. Choi , and M. S. Suh, Material characteristics of an ER fluid and its influence on dampingforces of an ER damper, *Part I: material characteristics, Materials & Design*, 20(6), (1999) 317-323.

[7] W. C. Park , S. B. Choi , and M. S. Suh, Material characteristics of an ER fluid and its influence on dampingforces of an ER damper, *Part II: damping forces, Materials & Design*, 20(6), (1999) 325-330.

[8] S. B. Choi, and Y. T. Choi, Sliding Model Control of a Shear-Mode Type ER Engine Mount, *KSME Int. J.*, 13(1), (1999) 26-33.

[9] J. D. Carlson, and K. D. Weiss, A growing attraction to magnetic fluids, *J. Machine Design*, 66(15), (1994) 61-64.

[10] J. D. Carlson, and M. J. Chrzan, Magnetorheological Fluid Dampers, U.S. Patent 5277281, 1994.

[11] R. Boelter, and H. Janocha, Performance of longstroke and low-stroke MR fluid damper, Proc. Of SPIE, Smart Structures and Materials: Passive Damping and Isolation, San Diego, CA, (1998) 303-313.

[12] S. J. Dyke, B. F. Spencer, Jr, M. K. Sain, and J. D. Carlson, Modelling and control of magnetorheological fluid dampers for seismic response reduction, *Smart Material and Structures*, 5, (1996) 565-575.

[13] S. R. Hong, S. B. Choi, Y. T. Choi, and N. M. Wereley, Non-dimensional analysis and design of a magnetorheological damper, *J. of Sound and Vibration*, 288(4), (2005) 847-863.

[14]S. S. Yoon, S. C. Kang, S. K. Yun, S. J. Kim, Y. H. Kim, and M. S. Kim, Safe Arm Design with MRbased Passive Compliant Joints and Visco-elastic Covering for Service Robot Applications, *KSME Int. J.*, 19(10), (2005) 1835-1845.

[15] K. M. Choi, H. J. Jung, S. W. Cho, and I. W. Lee , Application of smart passive damping system using MR damper to highway bridge structure, *KSME Int. J.*, 21(6), (2007) 870-874.

[16] M. Ahmadian, and J. A. Norris, Experimental analysis of magneto-rheological dampers when subjected to impact and shock loading, *Communications in Nonlinear Science and Numerical Simulation*, 13(9), (2008) 1978-1985.

[17] G. Aydar, C. A. Evrensel, F. Gordaninejad, and A.Fuchs, A Low Force Magneto-rheological (MR) Fluid Damper: Design, Fabrication and Characterization, *J. of Intelligent Material Systems and Structures*,18(12), (2007) 1155-1160.

[18] C. Spelta, F. Previdi, S. M. Savaresi, G. Fraternale, and N. Gaudiano, Control of magnetorheological dampers for vibration reduction in a washing machine, *Mechatronics*, (2008) Article in press.

[19] R. Stanway, J. L. Sproston, and N. G. Stevens, Non-linear Modelling of an Electro-rheological Vibration Damper, *J. of Electrostatics*, 20(2), (1987) 167-184.

[20] D. R. Gamota, and F. E. Filisko, Dynamic Mechanical Studies of Electrorheological Materials: Moderate Frequencies, *J. of Rheology*, 35(3), (1991) 399-425.

[21] B. F. Spencer, S. J. Dyke, M. K. Sain, and J. D.Carlson, Phenomenological Model of a Magneto-Rheological Damper, *ASCE J. of Engineering Mechanics*,123(3), (1996) 230-238.

[22] S. B. Choi, and S. K. Lee, A Hysteresis Model for the Field- dependent Damping Force of a Magnetorheological Damper, *J. of Sound and Vibration*,245(2), (2001) 375-383.

[23] A. Dominguez, R. Sedaghati, and I. Stiharu, Modelling the hysteresis phenomenon of magnetorheological dampers, *Smart Materials and Structures*, 13(6), (2004) 1351–1361.

[24] A. Dominguez, R. Sedaghati, and I. Stiharu, Modeling and application of MR dampers in semiadaptive structures, *Computers and Structures*, 86(3), (2008) 407–415.

[25] N. M. Kwok, Q. P. Ha, T. H. Nguyen, J. Li, B. Samali, A Novel Hysteretic Model for Magneto-Rheological Fluid Damper and Parameter Identification Using Particle Swarm Optimization, *Sensorand actuators A: Physical*, 132(2), (2006) 441-451.

[26] N. M. Kwok, Q. P. Ha, M. T. Nguyen, J. Li, and B.Samali, Bouc-Wen Model Parameter Identification for a MR Fluid Damper Using Computationally Efficient GA, *ISA transactions*, 46(2),(2007) 167-179.

[27] C. C. Chang, and P. Roschke, Neural network modelling of a magnetorheological damper, *J. Intell. Mater.Syst. Struct.*, 9(9), (1998) 755-764.

[28] K. C. Schurter, and P. N. Roschke, Fuzzy Modelingof A Magneto-Rheological Damper Using Anfis, Proc. of IEEE Int. Conf. on Fuzzy Systems, (2000) 122-127.

[29] D. H. Wang, and W. H. Liao, Neural Network Modeling and Controllers for Magneto-rheological Fluid Dampers, Proc. of 10th IEEE Int. Conf. On Fuzzy Systems, (2001) 1323-1326.

[30] D. H. Wang and W. H. Liao, Modeling and Control of Magneto-Rheological Fluid Damper Using Neural Networks, *Smart Materials and Structure*, 14(1), (2005) 111-126.

[31] I. H. Shames, and F. A. Cozzarelli, Elastic and Inelastic Stress Analysis, Prentice Hall, Englewood Cliffs, New Jersey, (1992) 120-122. [32]L. X. Wang, A Course in Fuzzy Systems and Control, Prentice Hall, 1997.

[33] M. P. Kevin, Y. Stephen, Fuzzy Control, Addison Wesley Longman, Menlo Park, CA, 1998.